Application of Particle Swarm Optimisation to evaluation of Polymer Cure Kinetics Models

T. Tilford [1], M. Ferenets [2], J. E. Morris[3], A. K. Parrott [1], A. Krumme[4], M. P. Y. Desmulliez [5] and C. Bailey [1]

[1] University of Greenwich, Greenwich, London SE10 9LS, United Kingdom

[2] Eesti Innovatsiooni Instituut, Sepapaja 6, Tallinn 11415, Estonia

[3] Portland State University, Portland, OR 97207-0751, USA

[4] Tallinn University of Technology, Ehitajate tee 5, Tallinn 19086, Estonia

[5] Herriot-watt University, Edinburgh, EH14 4AS, United Kingdom

Email: T.Tilford@gre.ac.uk

1. ABSTRACT

A particle swarm optimisation approach is used to determine the accuracy of six disparate cure kinetics models in order to determine their accuracy. The cure processes of two commercially available thermosetting polymer materials utilised in microelectronics manufacturing applications have been studied using a differential scanning calorimetry system. Numerical models have been fitted to the experimental data using a particle swarm optimisation algorithm which enables the ultimate accuracy of each of the models to be determined. The particle swarm optimisation approach to model fitting is has proved to be relatively rapid and is effective in determining optimal coefficient set for the cure kinetics models assessed. Results indicate that the single-step autocatalytic model is able to represent the curing process

more accurately than more complex model, with ultimate accuracy likely to be limited by inaccuracies in processing of the experimental data.

2. INTRODUCTION

The Controlled Collapse Chip Connection package (also referred to as a ‘flip chip’) is a means of connecting a semiconductor die to a printed circuit board and, hence, to other components in an electronics assembly. Such packages are widely used to package high performance semiconductor devices and enable high density assemblies essential to modern electronics devices. A flip-chip package consists of a silicon die with a large number of metallic pads arranged on the upper surface. Small solder balls are deposited on these pads. The device is then flipped over so the pads and solder balls face downward. The assembly is the placed onto a circuit board that has matching pads. The space between the circuit board and the silicon die is filled with a thermosetting polymer material known as an ‘underfill’ to provide mechanic support to the silicon die. The whole package is then covered with a second thermosetting polymer material encapsulant material to protect it from environment factors such as moisture, humidity and to provide electrical insulation. Fig 1 diagrammatically represents a cross section of a flip-chip package. The underfill and encapsulant materials are applied in a liquid state and are heated to induce the cure process. Incomplete cure of the underfill or encapsulant can be detrimental to the thermomechanical properties and can lead to failure modes such as de-lamination between material interfaces. There is therefore a requirement to ensure that the materials are fully cured.

In order to determine the degree of cure of polymer materials, two experimental approaches are typically used. Differential Scanning Calorimetry (DSC) equipment can be used to analyse the energy flux from a sample as it is heated. Alternatively, Fourier Transform Infra-Red (FTIR) spectroscopy can be used to determine the molecular composition of a test sample. However, neither of these approaches is applicable to in-situ measurement of degree of cure in practical applications.

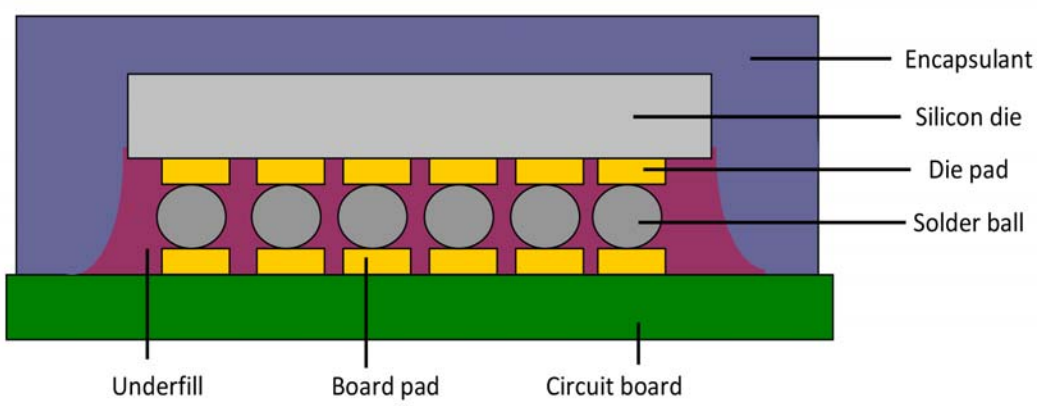

Figure 1; Cross section of a flip chip package

3. Polymer cure process

Thermosetting polymers materials are a subset of polymers, in which the interlinking of the polymer chain is irreversible. Polymer materials consist of a very large number of basic structural units (known as monomers) which are interconnected to form a large macromolecule. The fundamental structure typically consists of a long chain of monomers which become entangled and interlinked. The manner in which this interlinking occurs at the mesoscopic scale has a significant influence of the macroscopic material properties. The cross-linking process is initiated through addition of heat energy which causes the polymer chain to link into a highly complex

three-dimensional structure. Multiple polymer chains can interlink together, resulting in union of many polymers molecules. The process of molecular interlinking is referred to as ’curing’. The ’degree of cure’ is a measure of the proportion of the interlinking process that a material has undergone. It is possible to determine the exact molecular state of a polymer using techniques as Fourier Transform InfraRed Spectroscopy (FTIR) and Raman spectroscopy. As the curing of thermoset materials is generally exothermic, the degree of cure is often linked to the proportion of energy released by the material. This relation was initially proposed by Sourour [1]. The proportion of heat released by a polymer material can be determined through use of Differential Scanning Calorimetry (DSC) and this technique has been most widely adopted in analysis of polymer curing.

A large body of research focuses on attempting to describe the curing process, in particular, the rate of cure, in terms of material temperature. Initial work on thermosetting polymers was based on the work of Svante Arrhenius [2] who proposed that the rate of reaction (k) in a chemical system could be described empirically by; $k = A \exp(E/RT)$, in which A was a rate constant , E was an activation energy, R was the gas constant and T is the material temperature. The relation, which was initially proposed by Jacobus Henricus van ’t Hoff five years prior to Arrhenius’ interpretation of it, underpinned early understanding of chemical reactions. In order to determine the rate of cure of a polymer material using Arrhenius’ equation, an estimate of the rate constant A and the activation energy E are required.

4. CURE KINETICS MODELS

Many variations of the basic Arrhenius model have been proposed and assessed. A review of cure kinetics methods has been published by Yousefi et al [3], while an overview of modelling is presented by Morris et al [4]. The most general formulation of cure kinetics models is the nth order phenomenological model. The degree of cure can either be determined algebraically for constant heating rates or through numerical integration. For α= degree of cure, the basic assumption of all models is that the reaction rate can be expressed in terms of the temperature dependent chemical 'rate constant', K, which is a function of temperature, and a function, f(α), of reactant concentration at absolute temperature, T, as

$$\frac{\delta\alpha}{\delta t} = K \cdot f(\alpha) = \mathrm{A} \cdot \exp^{\left[\frac{-\mathrm{E}}{\mathrm{RT}}\right]} \cdot f(\alpha) \qquad (1)$$

Reaction rate parameters A and activation energy E are assumed to be characteristic constants of the polymer, and R=8.31J/K.mole. Cure models vary in the assumed form of f(α), with two predominant forms; the nth order form and the autocatalytic form. The nth order models assume $f(\alpha) = (1 - \alpha)^n$ and, in these cases, one can find α analytically for constant T, (i.e. isothermal cure) using equations 2 to 4 for 1st order, 2nd order and nth order models respectively.

$$\frac{\delta\alpha}{\delta t} = K(1-\alpha) \;\; \therefore \;\; \alpha = 1 - e^{(-Kt)} \qquad (2)$$

$$\frac{\delta\alpha}{\delta t} = K(1-\alpha)^2 \;\; \therefore \;\; \alpha = 1 - [1+Kt]^{-1} \qquad (3)$$

$$\frac{\delta\alpha}{\delta t} = K\left(1-\alpha\right)^{n} \quad \therefore \quad \alpha = 1-[1+\left(\left(n-1\right)Kt\right)]^{-1/(n-1)} \tag{4}$$

The autocatalytic models consist of the single-step model given in equation 5, the double step given in 6 and the modified double step, given in 7. The nth order models are based on the simple notion that the reaction rate is proportional to the un-reacted reagent mass available. The single step autocatalytic model, given in equation 5, is based on the concept that the reaction proceeds at the boundary of reacted and un-reacted material and is activated by an exothermic reaction. Note, however, that dα/dt=0 for α=0, which is non-physical and leads to "starting" problems.

The double-step auto-catalytic model (equation 6) is designed to solve this problem, but the single n-exponent does not suggest two independent reactions. However, it is the only model with more than a single chemical rate constant, i.e. all others implicitly assume a single chemical curing reaction, or at least a single rate controlling reaction across the full temperature range of interest. (The modified double-step, given in equation 7, provides two reaction rates, but with a single activation energy.

$$\frac{\delta\alpha}{\delta t} = K\ \alpha^{m}\ (1-\alpha)^{n} \tag{5}$$

$$\frac{\delta\alpha}{\delta t} = (K_1 + K_2\alpha^{m})(1-\alpha)^{n} \tag{6}$$

$$\frac{\delta\alpha}{\delta t} = K(y_1 + y_2\alpha^{m})(1-\alpha)^{n}\ ;\ y_1 + y_2 = 1 \tag{7}$$

5. TRADITIONAL MODEL-FITTING APPROACHES

Initial work to determine cure kinetics model coefficient sets for thermosetting polymer materials was carried out by Ozawa et al. This seminal research focused on thermal analysis of materials to determine reaction rates. A large body of work has been published by the author [5 - 8] and a number of other researchers have analysed Ozawa's contribution to the field, e.g. [9]. The Ozawa method for obtaining cure kinetics parameters, which is well outlined in [10], assumes that the degree of cure is proportional to the reaction exotherm. DSC analysis of the material is performed at a minimum of two disparate constant heating rates. A relation proposed by Doyle et al [11] defined an approximation for the cure rate for $E/RT < 20$. Ozawa utilised the Doyle approximation to form a set of equations for multiple heating rates in which the actual cure function cancelled out. This enables the values of the activation energy and subsequently the rate constant to be determined. The accuracy of the model is reliant on the accuracy of the Doyle approximation, but has been utilised readily since its proposal. The Ozawa approach can be used to determine the Activation Energy, E, from the relationship given in 8, in which β is the heating rate, R is the gas constant and T_p is the peak temperature. A popular alternative to the Ozawa method is the Kissinger equation [12] which activation energy and rate constant, A, can be determined from relations given in 9 and 10.

$$E = \frac{R}{1.502} \frac{\Delta \ln \beta}{\Delta\left(1/T_p\right)} \tag{8}$$

$$E = -R\frac{\partial\left(\ln\left(\beta / T_p^2\right)\right)}{\partial\left(1/T_p\right)} \tag{9}$$

$$A = \frac{\beta E \exp\left(E / RT_p\right)}{RT_p^2} \tag{10}$$

6. PARTICLE SWARM OPTIMISATION

The cure kinetics models can be applied to a range of thermosetting polymer materials. The model coefficients are varied in order to fit a model to a particular material. A number of approaches have been proposed for determining the optimal coefficient set for polymer materials. However, traditional approaches rely on a number of assumptions which may not be applicable to rapid cure processes. To overcome these issues, a particle swarm optimisation algorithm has been developed to determine optimal model coefficients in response to sets of experimentally derived cure data. This approach has been used previously for cure kinetics studies by Pagano et al [13] and by Ourique et al [14], although not applied to complex multi-component materials such as those assessed in this study.

Particle Swarm Optimisation (PSO) [15] is a stochastic optimisation approach based on the concept of 'swarm intelligence'. The PSO algorithm defines a large number of particles occupying multi-dimensional space. Each of the hyperspace dimensions relates to a cure model parameter, so the position of each particle relates to a set of model parameters. The accuracy of the model at each coefficient set can be determined by comparing the cure process predicted by the model with experimentally derived data. Once the accuracy, typically referred to as 'fitness', has

been determined, the velocity of the particles is updated based on the fitness of each particle relative to it's own fitness compared to the optimal value found by any of the particles in the swarm. The optimisation algorithm then proceeds in an iterative manner, with each particle considering its own optimal position as part of the velocity update, until it is decided that a sufficiently converged solution has been obtained.

The steps required in the particle swarm algorithm are:

Initialise particle positions, particle velocities, local fitness and global fitness

$$x_i \in U(x\min_i, x\max_i)$$
$$v_i = 0$$
$$\hat{f}_i = \infty$$
$$\hat{f}_{global} = \infty$$

Iterative progression while $k \leq k_{max}$

Calculate fitness for each particle $$f_i = \int_0^{\infty} \sqrt{\left(\frac{\partial \alpha_m}{\partial t}\right)^2 - \left(\frac{\partial \alpha_e}{\partial t}\right)^2}\, dT$$

Update particle optimum position $$\hat{x}_i = x_i \text{ if } f_i < \hat{f}_i$$

Update global optimum position $$\hat{g} = x_i \text{ if } f_i < \hat{f}_{global}$$

Update particle velocity $$v_i = \omega v_i + c_1 r_1 (\hat{x}_i - x_i) + c_2 r_2 (\hat{g} - x_i)$$

Update particle position $$x_i = x_i + v_i$$

In this description, there are i particles and j hyperspace dimensions, with x_i being the position vector of particle i and v_i being the velocity vector of particle i. The fitness, f_i, of each particle is based on a root mean square error metric of the difference between the transient cure behaviour of the model, α_m and the experiment data, α_e. The global optimum and particle optimum positions are designated $\hat{g}$ and $\hat{x}_i$ respectively, the particle optimal fitness is $\hat{f}_i$ while the global optimal fitness is $\hat{f}_{global}$. Algorithm coefficients ω, c_1 and c_2 represent particle momentum, particle optimum attraction and global optimum attraction respectively while r_1 and r_2 are random values $\in U(0,1)$. The algorithm proceeds iteratively from k = 1 to k = k_{max}. The values used in the analyses are detailed in table I.

Parameter	Symbol	Value
Number of particles	i	100000
Number of hyperspace dimensions	j	6
Number of iterations	k	20
Particle momentum	c_1	0.02
Particle optimum attraction	c_2	2.00
global optimum attraction	ω	0.05

Table I: Particle Swarm Optimisation parameters

The progression of the particles from their initial uniform distribution over the hyperspace to an optimal point is illustrated in figures 1 to 6 on the following page. The case is a first order model in which only two parameters (activation energy E and rate constant A) are considered. The particles rapidly move toward the optimal values in each of the dimensions and then slowly move toward the two dimensional optimal point. If the algorithm was allowed to continue, all particles would eventually occupy a single point in the hyperspace. The algorithm has been implanted in Fortran 90 and parallelised with OpenMP [16] directives to run on a 16 core AMD Opteron 8354 system. Runtimes obviously vary dependant on experimental data, model analysed and runtime setting but analysis of the accuracy of the single step model against five experimental data sets takes approximately 1027 seconds.

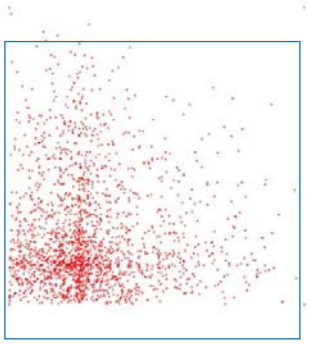

Figure 1. Particle distribution; k = 1

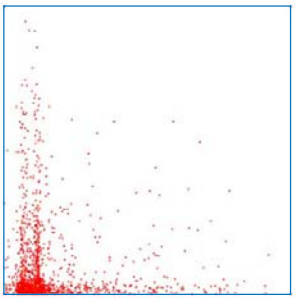

Figure 2. Particle distribution; k = 2

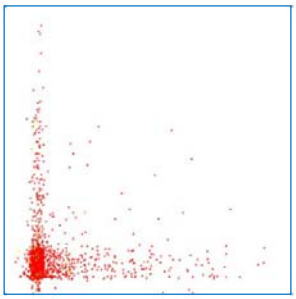

Figure 3. Particle distribution; k = 3

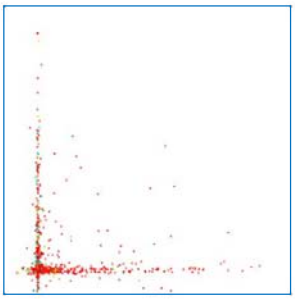

Figure 4. Particle distribution; k = 5

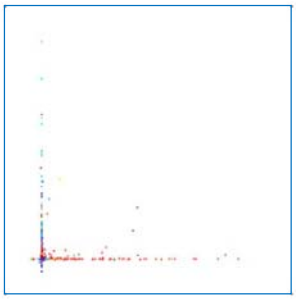

Figure 5. Particle distribution; k = 18

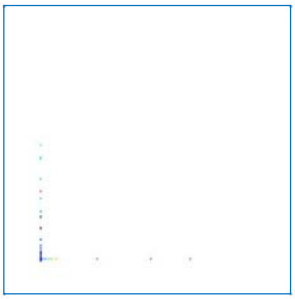

Figure 6. Particle distribution; k = 500

7. DIFFERENTIAL SCANNING CALORIMETRY ANALYSIS OF TEST MATERIALS

In order to determine the actual cure behaviour of the sample materials, a series of experimental analyses were required. The objective of the experimental programme was to determine the variation in the degree of cure of the test materials with time and temperature. Two disparate materials were analysed; the first material being a commercially available encapsulant material Henkel Hysol® E01080, the second was an underfill material Henkel FP4511.

Differential scanning calorimetry (DSC) is an easy method for determining resin cure kinetics. DSC measures the heat flow into or from a sample as it is heated, cooled and/or held isothermally. For thermosetting resins like epoxies the technique provides information on glass transition temperature, T_g, onset of cure, heat of cure, maximum rate of cure, completion of cure and degree of cure.

A Perkin Elmer DSC-7 system was used for analysis of the samples in this study. Small amounts (typically 3 to 10 mg) of the sample materials were placed in aluminium crucibles and an empty crucible was used as a reference. Measurements were made in nitrogen atmosphere with a flow rate of 20 ml/min.

All materials used in these experiments are one component epoxy resins. This means that epoxy and its hardener are already mixed together, but the curing is prevented by keeping the mixture at low temperature (at +5 ^{o}C for EO1080 and at -40 ^{o}C for FP4511). The cure profiles recommended by the material manufacturer are presented in Table II.

One of the aims of this study was to assess the applicability of these models for microwave curing processes. The series of temperature profiles, listed in tables III and IV, were developed for the tests, with high curing rates intended to mimic temperature profiles characteristic of microwave curing.

Material	Suggested temperature, ºC	Curing time
EO1080	110 degrees 140 degrees 150 degrees	2 hours 1.5 hours 20 min
FP4511	150 degrees	2 hours

Table II: Curing methods of tested materials suggested by Henkel

Profile number	Start Temp ºC	Final Temp ºC	Ramp rate ºC/min
1	20	300	150
2	20	300	200
3	20	300	100
4	0	300	50
5	0	300	10

Table III: Temperature profiles for encapsulant tests

Profile number	Start Temp °C	Final Temp °C	Ramp rate °C/min
1	0	300	20
2	0	300	10
3	0	250	20 (750 s) 0 (180 s)
4	0	250	30

Table IV: Temperature profiles for underfill tests

8. RESULTS

DSC analysis of the sample materials was performed in order to provide energy flux data. As the material consists of a mix of polymers, fillers and solvents, the energy flux during cure is a complicated compound result of multiple reactions. The DSC data therefore required processing to separate the exothermal polymer cure reaction from the tertiary reactions. The pure DSC data for encapsulant sample 1 is presented in figure 7 as the blue line, with the cure energy flux (red line) defined as the difference between the pure data and an user-defined baseline (green). The degree of cure at any given time can be determined from the cumulative energy released compared with the total reaction energy. The variation of degree of cure with time for sample 1 is given in figure 8 while the cure rate is given in figure 9. The energy fluxes cure degree and cure rate variations have been determined for four further encapsulant samples and for five underfill samples

The numerical models have been used to predict transient development of degree of cure for the time-temperature profiles used during the DSC tests. The rate of cure has also been determined by the models and compared with experimental data.

The procedure has been repeated for the Henkel FP4511 underfill samples, with energy fluxes, cure rates, cure degree variation and numerical comparisons for the four samples plotted in figures 32 to 51. Results for CE3103 conductive adhesive material are presented in figures 52 to 76. Table VI to VIII present optimal model coefficients for all models used for each of the three materials, while figures 77 to 79 show the error for each model – material combination.

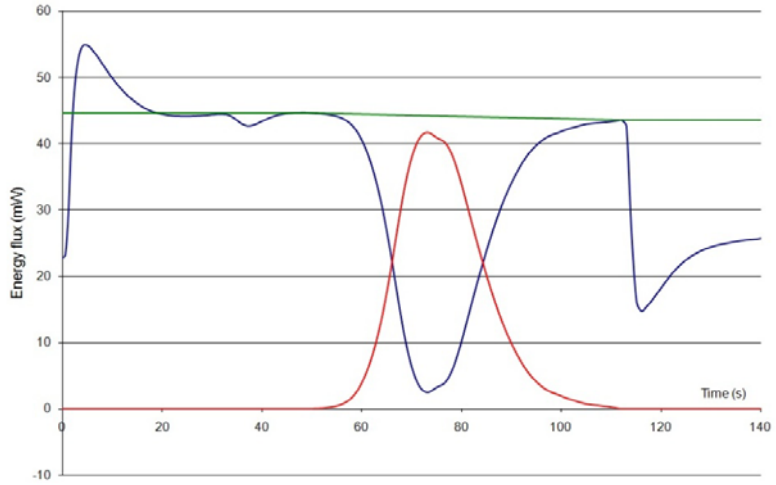

Figure 7 Energy flux for encapsulant test sample 1

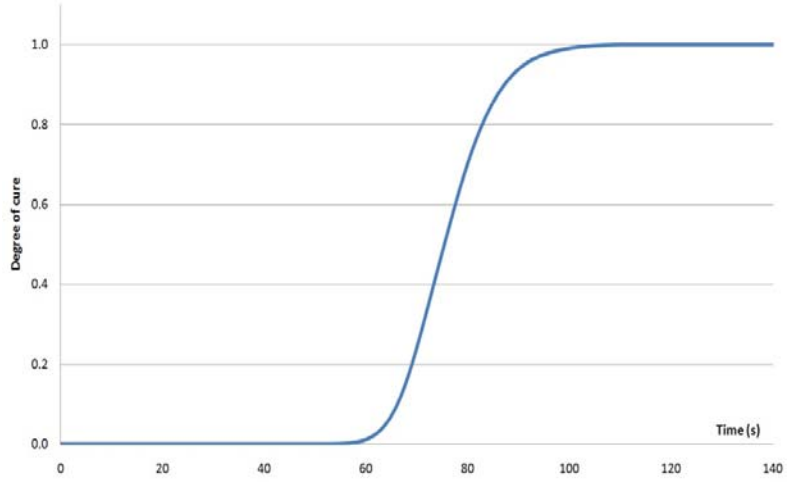

Figure 8 Variation in degree of cure for encapsulant test sample 1

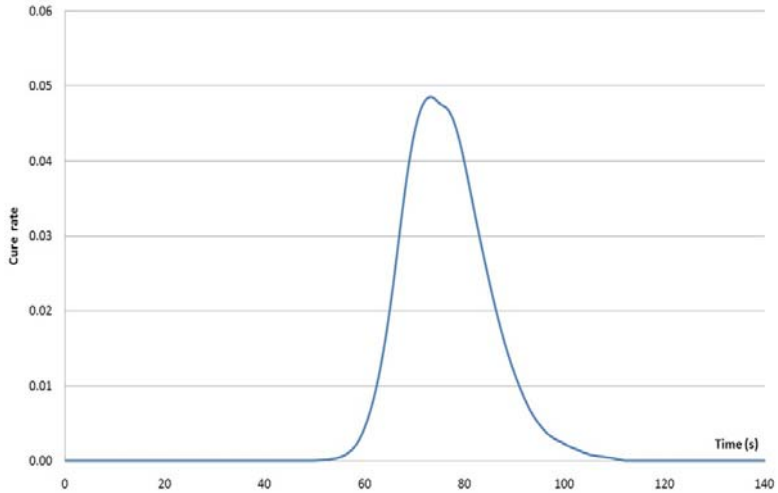

Figure 9 Variation in cure rate for encapsulant test sample 1

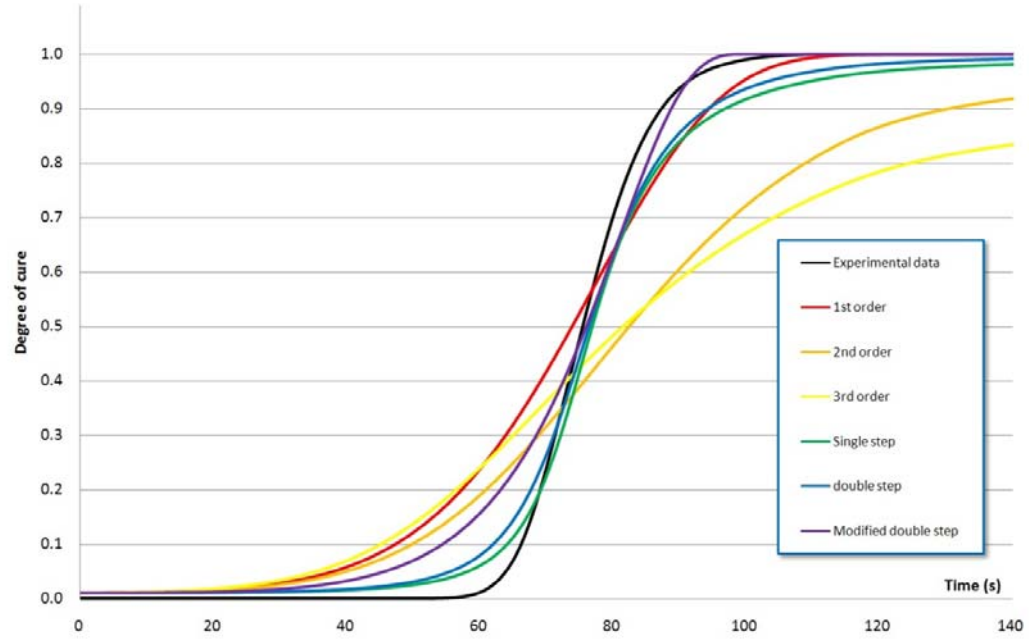

Figure 10 Comparison between experimental data and numerical solutions of cure process for encapsulant test sample 1

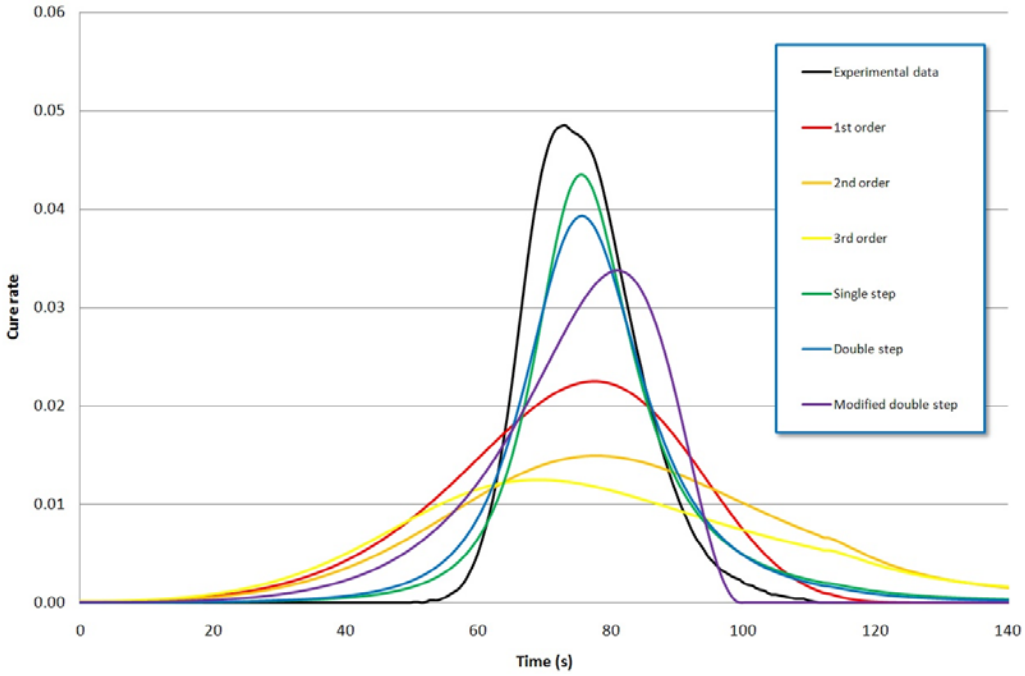

Figure 11 Comparison between experimental data and numerical solutions of cure rate for encapsulant test sample 1

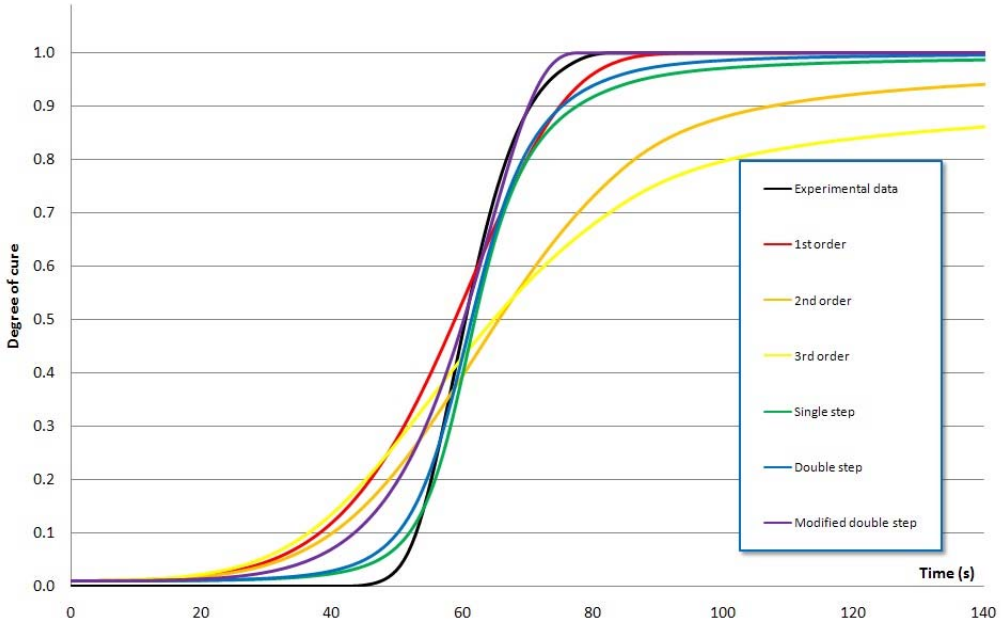

Figure 12 Comparison between experimental data and numerical solutions of cure process for encapsulant test sample 2

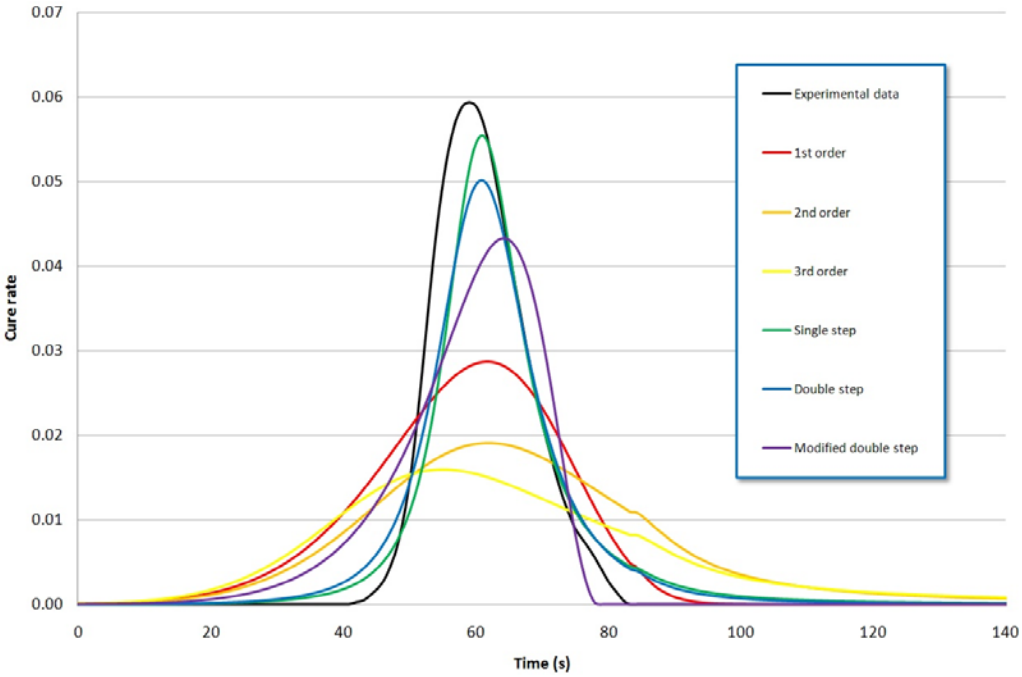

Figure 13 Comparison between experimental data and numerical solutions of cure rate for encapsulant test sample 2

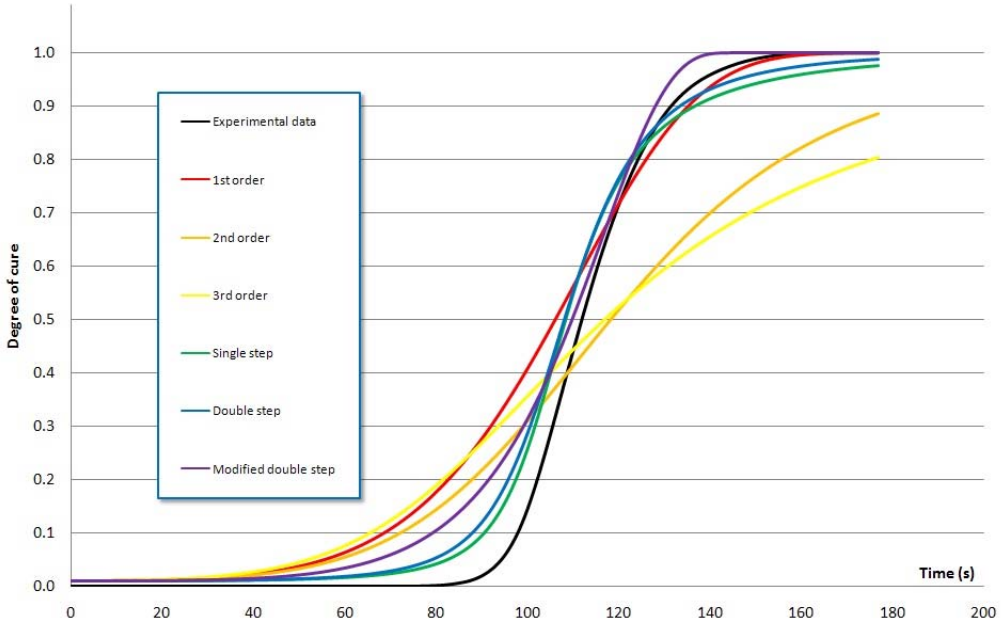

Figure 14 Comparison between experimental data and numerical solutions of cure process for encapsulant test sample 3

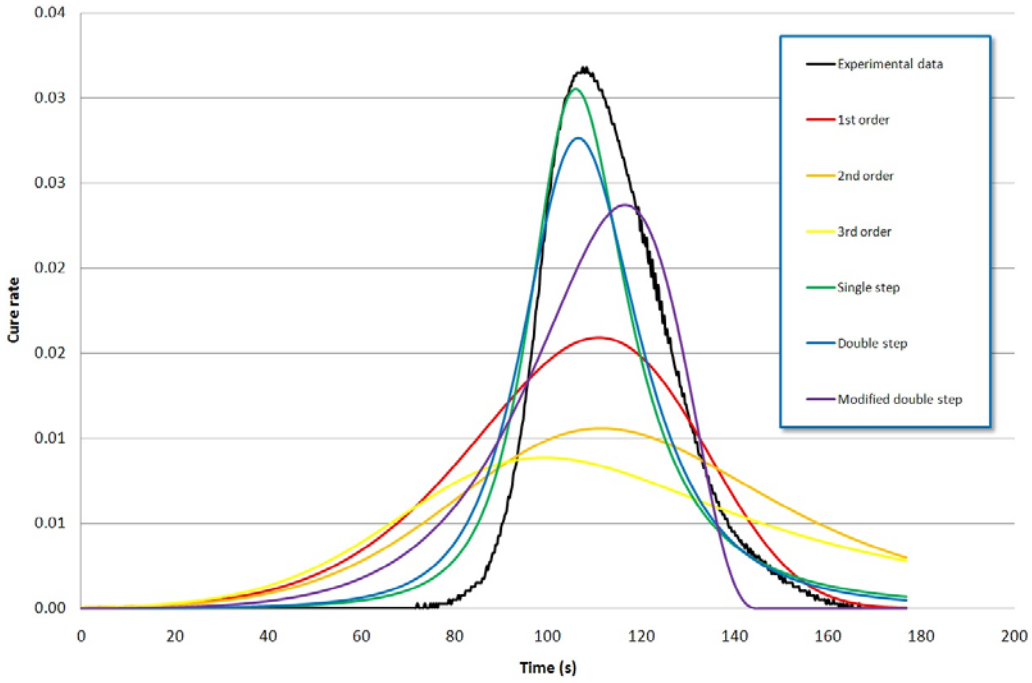

Figure 15 Comparison between experimental data and numerical solutions of cure rate for encapsulant test sample 3

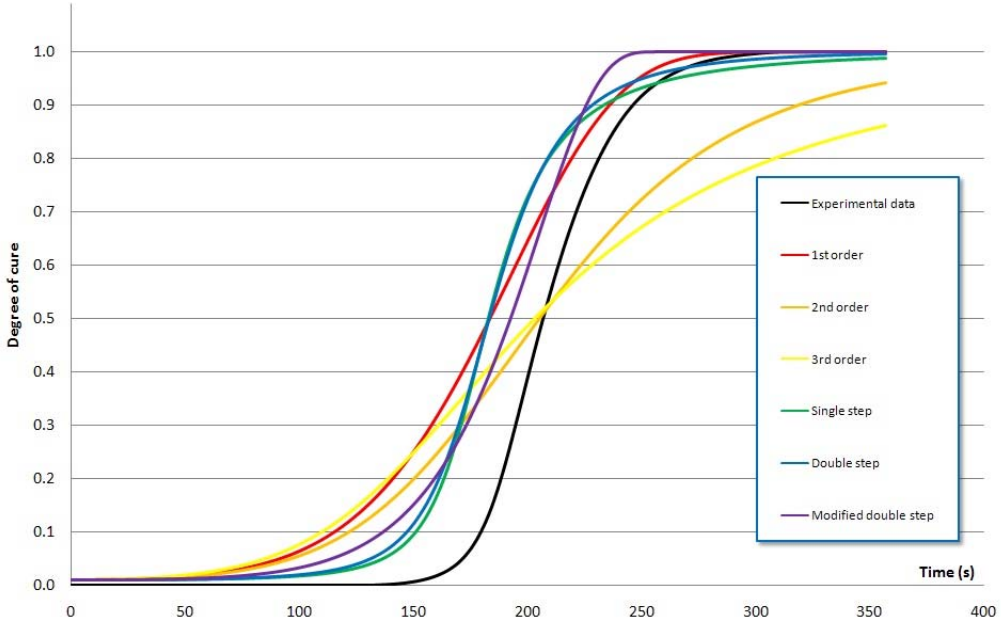

Figure 16 Comparison between experimental data and numerical solutions of cure process for encapsulant test sample 4

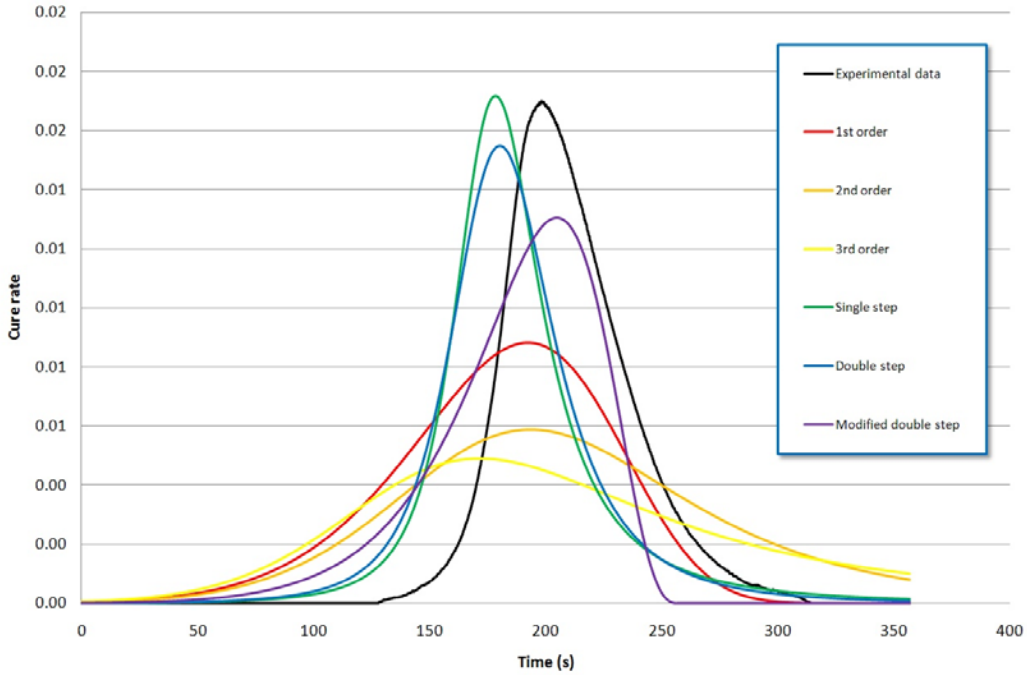

Figure 17 Comparison between experimental data and numerical solutions of cure rate for encapsulant test sample 4

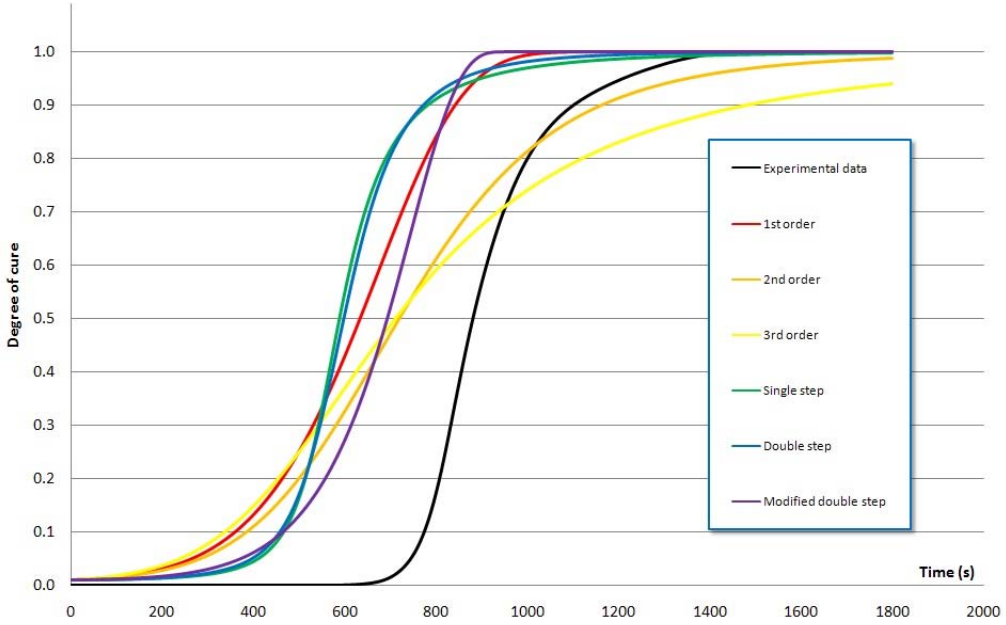

Figure 18 Comparison between experimental data and numerical solutions of cure process for encapsulant test sample 5

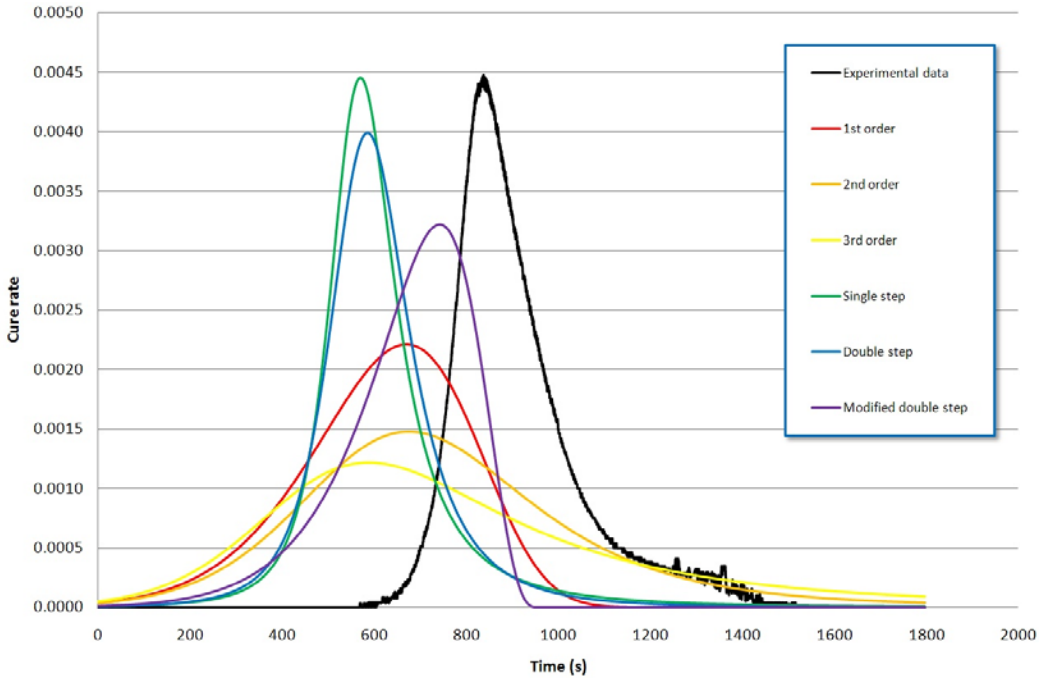

Figure 19 Comparison between experimental data and numerical solutions of cure rate for encapsulant test sample 5

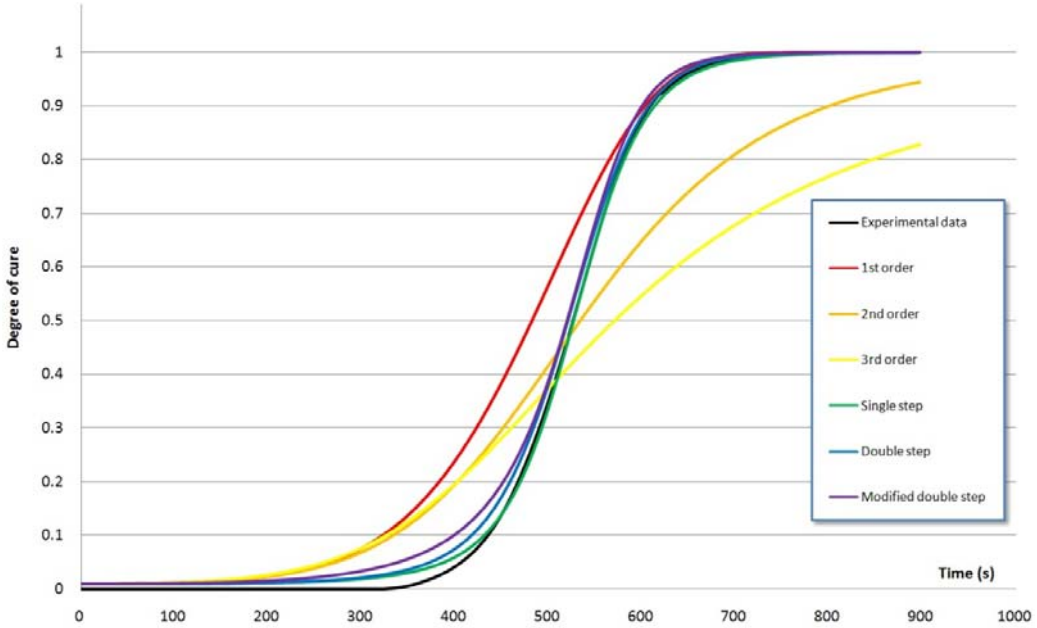

Figure 20 Comparison between experimental data and numerical solutions of cure process for underfill test sample 1

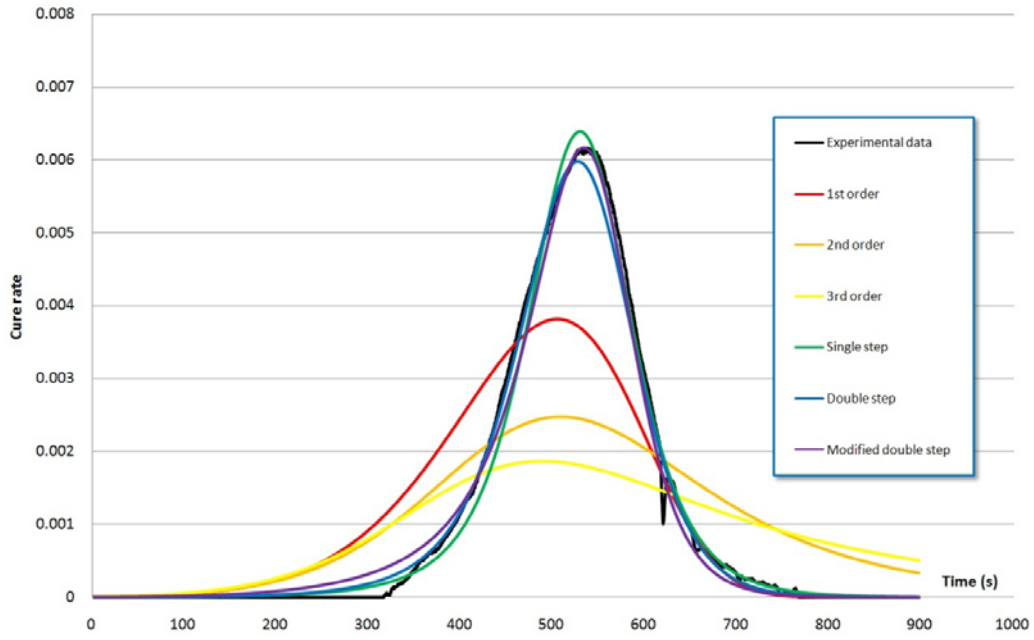

Figure 21 Comparison between experimental data and numerical solutions of cure rate for underfill test sample 1

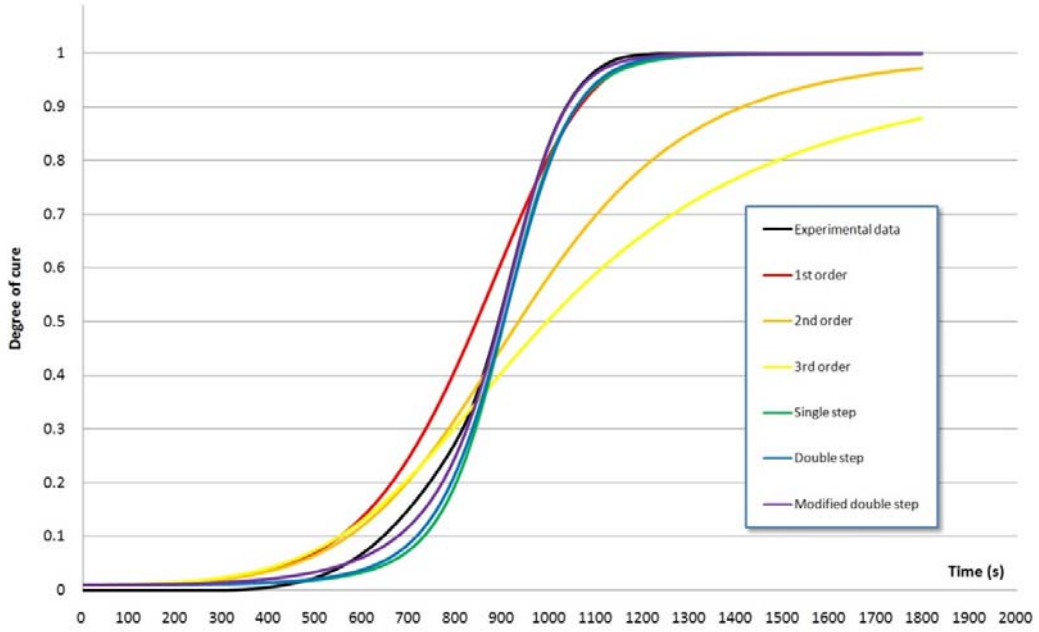

Figure 22 Comparison between experimental data and numerical solutions of cure process for encapsulant test sample 2

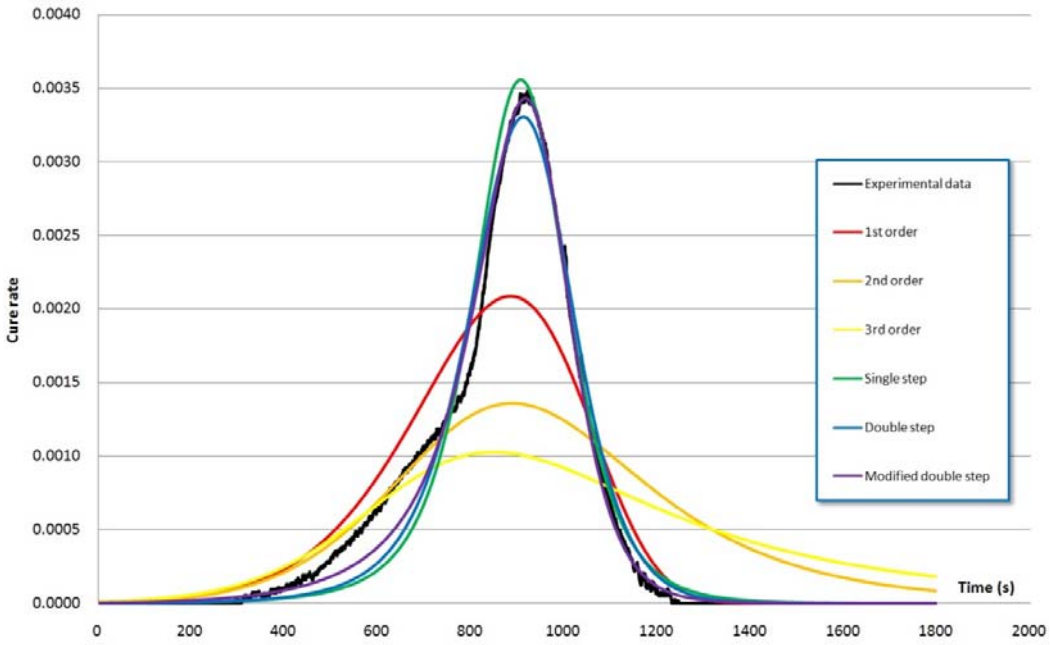

Figure 23 Comparison between experimental data and numerical solutions of cure rate for underfill test sample 2

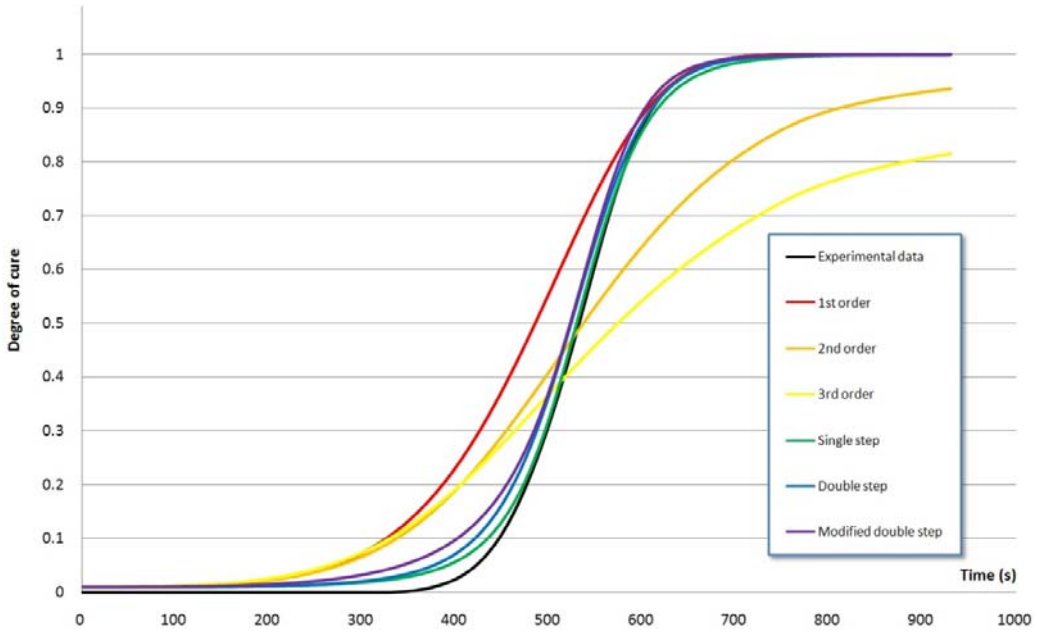

Figure 24 Comparison between experimental data and numerical solutions of cure process for underfill test sample 3

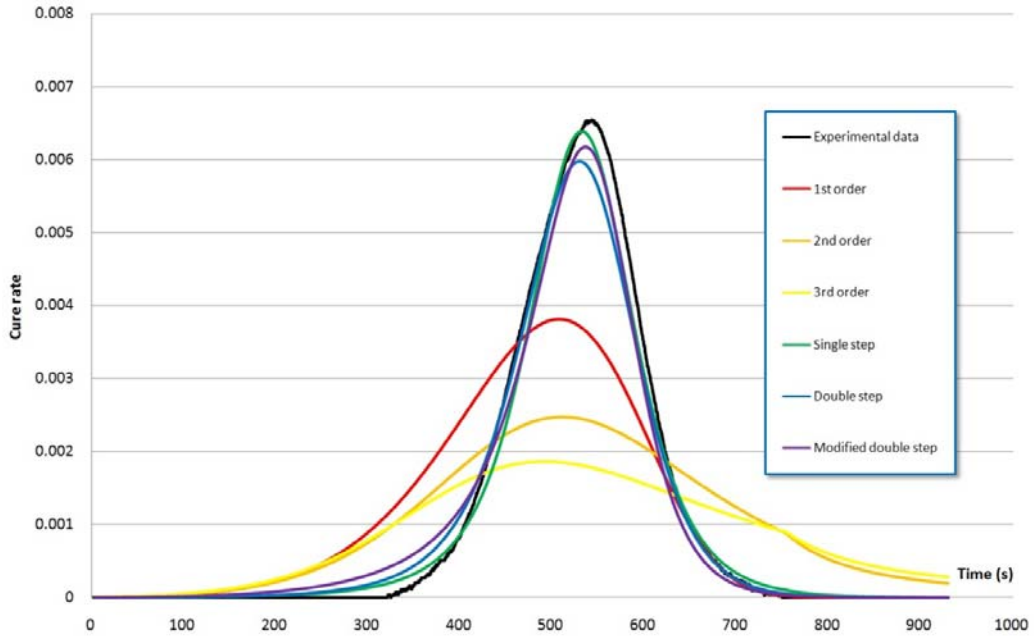

Figure 25 Comparison between experimental data and numerical solutions of cure rate for underfill test sample 3

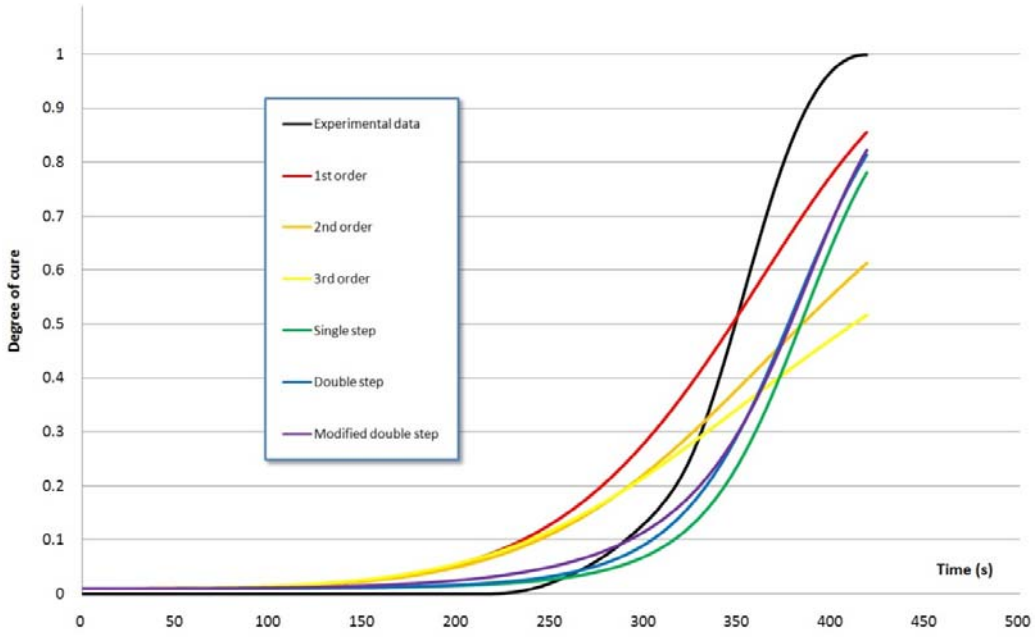

Figure 26 Comparison between experimental data and numerical solutions of cure process for underfill test sample 4

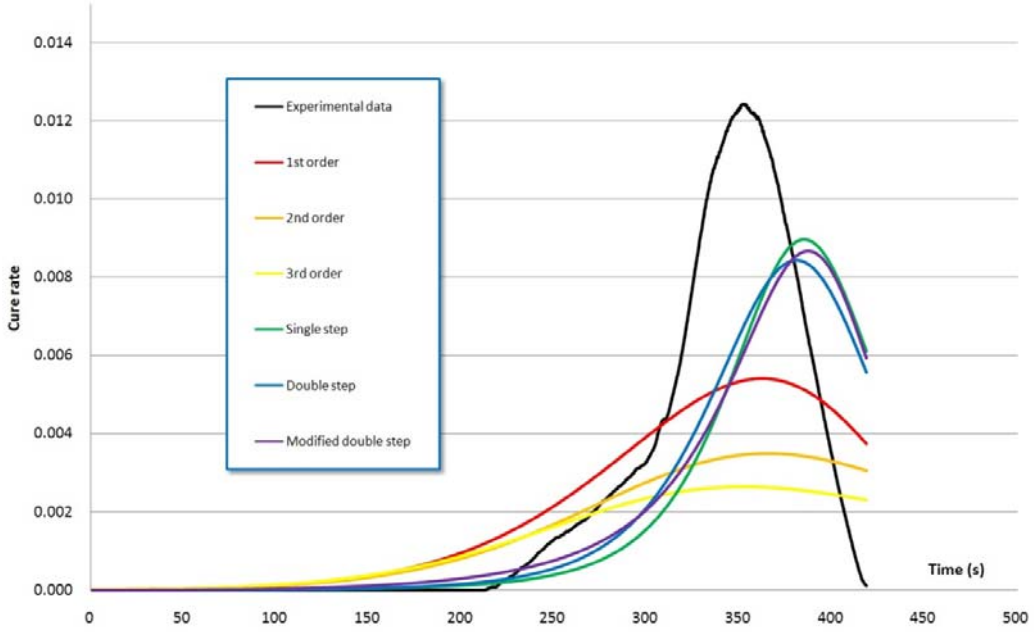

Figure 27 Comparison between experimental data and numerical solutions of cure rate for underfill test sample 4

Model	E1	A1	n	m	E2	A2	y1
1st order	39109.56	1075.40	1	-	-	-	-
2nd order	38947.38	875.53	2	-	-	-	-
3rd order	39071.93	1436.98	3	-	-	-	-
Single step	32493.47	1428.87	2.072	1.075	-	-	-
Double step	111995.69	322.90	1.761	0.915	33607.75	1295.48	-
Modified double	43519.70	2497.20	0.759	0.683	-	-	0.8007

Table V: Model coefficients for encapsulant data

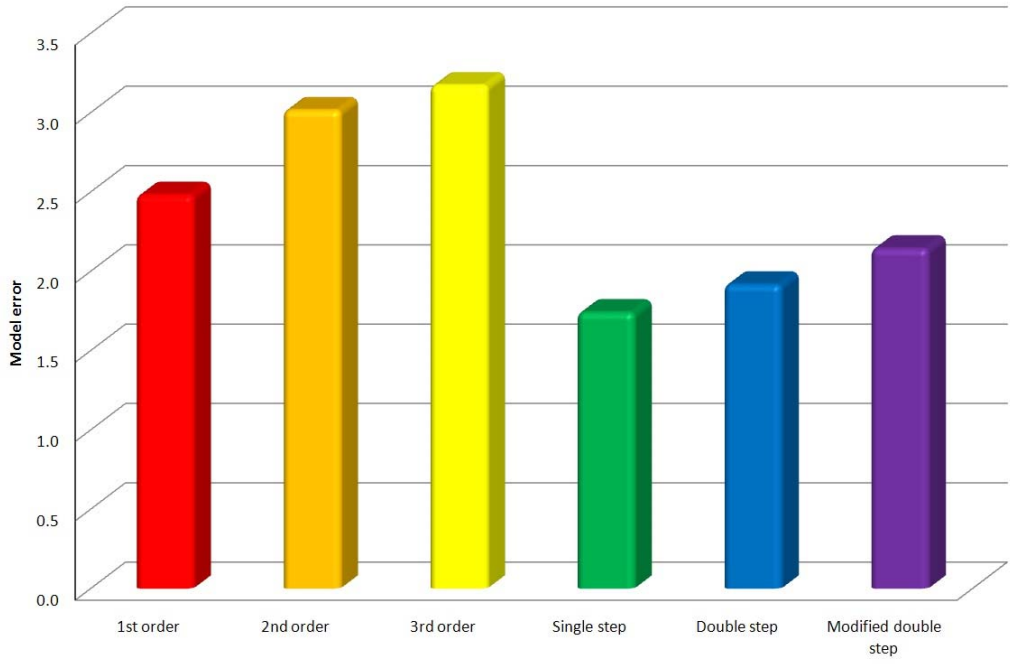

Figure 28 Error metric for the numerical models fitted to encapsulant data

Model	E1	A1	n	m	E2	A2	y1
1st order	44426.07	1658.29	1	-	-	-	-
2nd order	42793.06	874.61	2	-	-	-	-
3rd order	40893.34	544.72	3	-	-	-	-
Single step	36588.74	517.42	1.333	0.827	-	-	-
Double step	83933.39	542.86	1.208	0.679	39838.32	1000.76	-
Modified double	38237.14	643.49	1.133	1.078	-	-	0.0991

Table VI: Model coefficients for underfill data

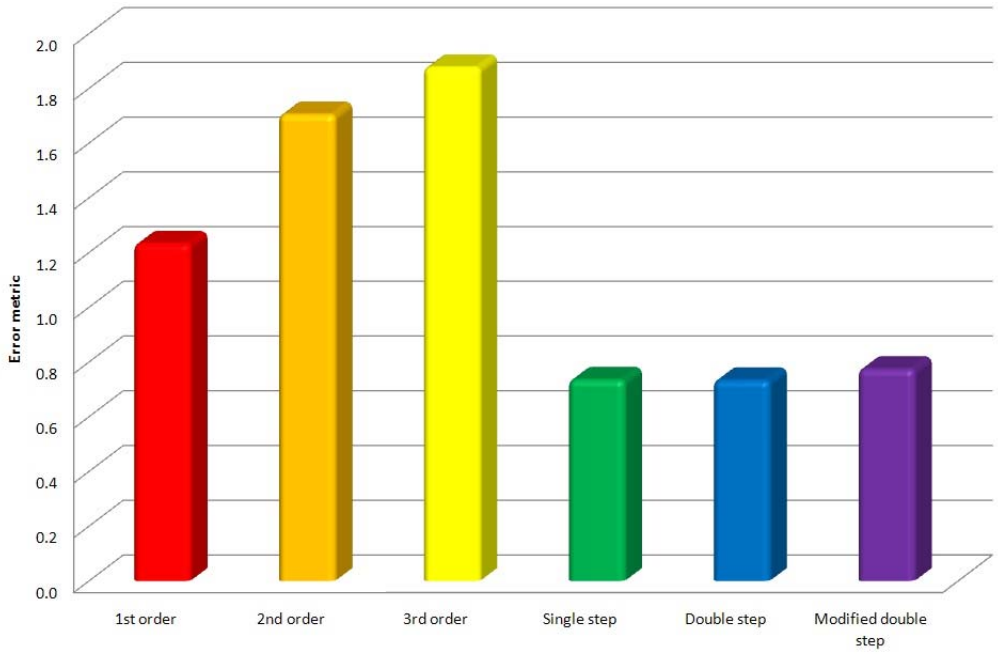

Figure 29 Error metric for the numerical models fitted to underfill data

9. CONCLUSIONS

The primary findings of this study are that the development of increasingly complex models does not necessarily lead to improvements in accuracy. The model fitting approach underpins the accuracy of the model, with the single step autocatalytic model providing a more accurate estimate of cure kinetics process than the more complex double step models.

The primary source of error in this study is considered to be the definition of the baseline DSC curve. This is currently determined through observation of the pure DSC data which leads to estimated times for the start and conclusion of the polymerisation process. The error in locating these points, combined with the assumption that the baseline is linear, is likely to exceed the inaccuracies of the cure kinetics models.

Further work is required to more accurately assess the cure process using Fourier Transform InfraRed spectroscopy. This will enable the proportion of primary, secondary and tertiary amines, enabling accurate separation of the exothermal processes from the reactions of the filler and solvents present within the material

10. ACKNOWLEDGMENTS

The authors wish to acknowledge funding and support from the European Union Framework 7 programme (FP7-SME-2007-2), contract number 218350 and additional support from our partners, Kepar Electronica S.A., Camero di Commercio Industria, Artigianato e Agricoltura di Milano, Mikrosystemtechnik Baden-Württemberg e.V., the National Microelectronics Institute, ACI-ecotec GmbH & Co. KG, Industrial Microwave Systems Ltd. and Ribler GmbH.

11. REFERENCES

1. Sourour, S. Thermal and Kinetic Characterization of Thermosetting Resins during Cure, PhD. Thesis, McGill University, 1978.
2. Arrhenius, S., Zeitschrift für Physikalische Chemie, 4: 226, 1889.
3. Lafleur, P.G., Yousefi, A. and Gauvin, R., Kinetic Studies of Thermoset Cure Reactions: A review. Polymer Composites, 18(2):157–168, 1997.
4. Morris, J. E., Tilford, T., Bailey, C., Sinclair, K. I., and Desmulliez, M. P. Y., 'Polymer Cure Modeling for Microelectronics Applications', Proceedings 32nd International Spring Seminar on Electronics Technology (ISSE 2009), Brno, Czech Republic, 2009.
5. Ozawa, T., A New Method of Analyzing Thermogravimetric Data. Bulletin of the Chemical Society of Japan 1965, 38(11), 1881–1886,
6. Ozawa, T., Kinetic Analysis of Derivative Curves in Thermal Analysis, Journal of Thermal Analysis and Calorimetry, 2(3):301 – 324, 1970.
7. Ozawa, T., and Kanari, K., Linearity and Non-linearity in DSC: A critique on modulated DSC. Thermochimica Acta, 253:183–188, 1995.

8. Ozawa, T., Thermal analysis review and prospect. Thermochimica Acta, 355(1-2):35-42, 2000.
9. Flynn, J. H., Early papers by Takeo Ozawa and their continuing relevance. Thermochimica Acta, 282-283:35 – 42, 1996.
10. Zetterlund, P. B. and Johnson A. F., A New Method for Determination of the Arrhenius Constants for the Cure Process of Unsaturated Polyester Resins based on a Mechanistic Model. Thermochimica Acta, 289(2):209 – 221, 1996.
11. C. D. Doyle. Estimating Isothermal Life from Thermogravimetric data. Journal of Applied Polymer Science, 6(24):639–642, 1962.
12. Kissinger H. E., 1957, Anal Chem, 29: 1702.
13. Tavares F. W., Pagano R. L., Calado, V. M. A. and Biscaia Jr., E. C., Cure Kinetic Parameter Estimation of Thermosetting Resins with Isothermal Data by using Particle Swarm Optimization. European Polymer Journal, 44:2678-2686, 2008.
14. Ourique, C.O., Biscaia, E.C., Pinto, J.C., The use of Particle Swarm Optimization for Dynamical Analysis in Chemical Processes. Comput Chem Eng 2002, 26(12), 1783–1793.
15. Clerc, M., Particle Swarm Optimization, Wiley Blackwell, 2006.
16. www.openmp.org